

Speed and Lifetime of Cosmic-Ray Muons: An Elucidation of Special Relativity and Weak Coupling Constant G_F

Chengchao Yuan*

Department of Physics, Pennsylvania State University, University Park, 16802, PA, USA

(Dated: Sep 22, 2016)

We present our measurements of mean speed and lifetime of cosmic-ray muons and show that muons are relativistic particles where classical mechanics based on Newton's laws are invalid. In particle physics, the decay time of muons can be exactly calculated using Fermi weak coupling constant G_F and rest mass, which enables us to link the lifetime given by experiment and the theory for weak interactions. In our work, we use scintillation detectors to record the pulses and use coincidence-analysis system to digitalize the time intervals. The average speed of muons is measured to be $1.58 \times 10^8 \text{m/s}$ (52.7% of light speed). The reasons of failure towards the speed and lifetime measurements are discussed. We also employ Monte Carlo simulations to discuss the broadening effect due to the momentum distribution of sea level muons. Since the atmospheric muons and their neutrinos play an important role in ground-based cosmic ray detectors, our methods can also be applied to construct the muon's track and energy loss inside these detectors and further the direction and energy of the incident astronomical particles can be inferred.

I. INTRODUCTION

I. 1 Cosmic Rays

Our Earth is immersed in the environment full of radiations and energetic particles, such as protons, alpha particles and neutrinos. The latter, named cosmic rays, are produced in the most violent astronomical processes inside or outside the Milky Way, according to contemporary observations and theories. Starforming and starburst galaxies which have a high occurrence rate of supernovae are the most promising sources and cosmic rays can be accelerated to 10^{21}eV through *Fermi* (shock) acceleration mechanism in supernova explosions[1]. Cosmic rays generated in the sources are called primary cosmic rays, of which protons dominate the particle species ($\approx 85\%$) followed by α particles ($\approx 12\%$) and heavier nuclei ($Z \geq 3, \approx 3\%$)[2]. During the propagation of charged particles before reaching the Earth, they are often influenced by the interstellar magnetic, as a consequence their trajectories are unpredictably distorted and the directional information is lost. This effect also leads to the isotropy of cosmic rays which enables cosmic rays to be a free and ideal source for particle experiments. However, when compared to the earlier prosperity of optical astronomy (in 17th century), it is generally believed that particle astrophysics was born with a remarkable finding about one century ago.

In 1912, Victor Hess sent a modified electrometer into the atmosphere along with a balloon to detect the ionization rate[3]. Before him, people believed the ionization and charged particles in the air came from radiative materials underground. If this projection is authentic, ionization should decrease with the height above the sea level. However, Hess' result was a dramatic surprise

because he found ionization at latitude 5300m increased approximately four times than sea level. In fact, when primary cosmic rays try to penetrate the atmosphere, they collide with atoms in the air and generate a particle cascade, called "air shower". Particles generated in this process are called secondary cosmic rays and the species are dramatically increased: pions, muons, kaons and their corresponding neutrinos, are produced. The lepton decay of pions and kaons produces relatively stable muons through these channels:

$$\pi^+ \rightarrow \mu^+ + \nu_\mu; \quad \pi^- \rightarrow \mu^- + \bar{\nu}_\mu$$

and

$$K^+ \rightarrow \mu^+ + \nu_\mu; \quad K^- \rightarrow \mu^- + \bar{\nu}_\mu.$$

In consequence, at sea level, almost 80% of secondary particles are muons. Accurate measurement of muon spectrum at sea level by Rastin (1984) gives the momentum spectrum that is illustrated in Figure 1. In our experiment, we will discuss the broadening effect contributed by the distribution of muons' momentum.

I. 2 Special Relativity

From the momentum spectrum, we can estimate the average momentum, which is $0.5 \text{GeV}/c$. In classical mechanics, the velocity is given by $v = p/m_\mu \approx 4.76c$, here we take $m_\mu = m_{\mu,0} = 0.105 \text{MeV}/c^2$. However, according to the special theory of relativity, the upper limit of speed is c , which implies that the relativistic effect cannot be ignored in this analysis. In relativistic mechanics, we have the relation between the speed and momentum

$$p = \frac{m_0 v}{\sqrt{1 - \frac{v^2}{c^2}}}, \quad (1)$$

* cxy52@psu.edu

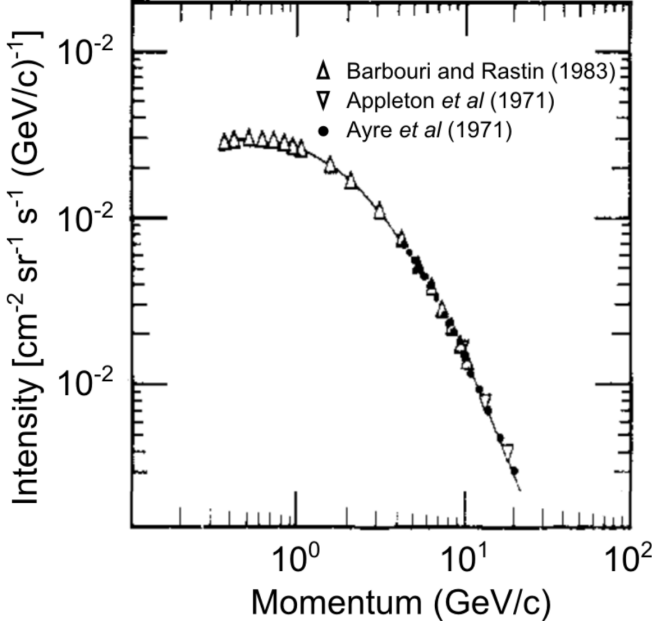


FIG. 1. The differential (in $\text{cm}^{-2} \text{sr}^{-1} \text{s}^{-1} (\text{GeV}/c)^{-1}$) momentum distribution of sea level muons[4] in vertical direction.

then we can solve the mean speed of muons in the unit of light speed $v_\mu = pc/\sqrt{m_0^2c^2 + p^2} \approx 0.979c$. Because most of the muons are produced in the top of atmosphere ($\approx 15\text{km}$), time required to arrive the earth would be at least $15\text{km}/c \approx 50\mu\text{s}$ which is much larger than the accepted muon lifetime $2.197\mu\text{s}$ [5]. To explain this phenomenon, we introduce the Lorentz transformation between two frames of reference (see appendix A). For a muon located at the original point in S' , the proper time interval in S would be

$$\Delta t' = \gamma \Delta t. \quad (2)$$

This is the relativistic dilation of time. Using $E = \gamma m_0 c^2$, we can find the relation between energy and distance before decaying

$$L = \tau c \sqrt{\left(\frac{E}{m_0 c^2}\right)^2 - 1}, \quad (3)$$

From this equation, muons with energy larger than 2.39GeV can travel 15 km before decaying to other particles.

I. 3 Lifetime of Muons

As the first unstable particle found by human[6], muon and its anti-particle, μ^+ , can decay through the following channels producing electrons/positrons and correspond-

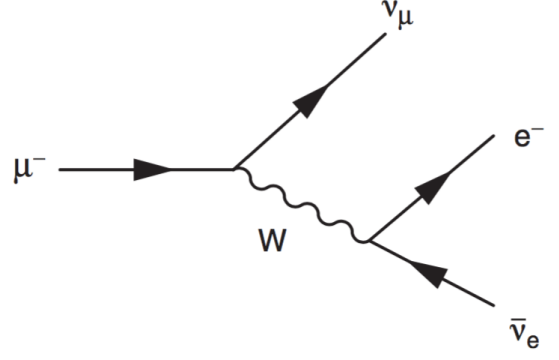


FIG. 2. Feynman diagram for μ^- decay that is mediated by the W boson: the muon decays to an electron, an electron antineutrino, and a muon neutrino. The positive time direction is rightward.

ing neutrinos:

$$\mu^- \rightarrow e^- + \bar{\nu}_e + \nu_\mu; \quad \mu^+ \rightarrow e^+ + \nu_e + \bar{\nu}_\mu$$

The Feynman diagrams this process can be found in figure 2,

The decaying process can be described by the lifetime τ such that

$$I(t) = I(0)e^{-t/\tau}, \quad (4)$$

where $I(0)$ and $I(t)$ are the number of muons at initial time and a duration t after that. According to Fermi's weak-decay theory, the lifetime τ of muons can be calculated directly using some basic parameters[7],

$$\frac{1}{\Gamma(\mu^- \rightarrow e^- \bar{\nu}_e \nu_\mu)} = \tau = \frac{192\pi^3}{G_F^2 m_\mu^5}, \quad (5)$$

where G_F is called Fermi decay constant which is related to the weak coupling strength (g_W) and W -Boson mass (m_W) through

$$G_F = \frac{\sqrt{2}g_W^2}{8m_W^2}. \quad (6)$$

Thus a precise measurement of muon lifetime can be used to determine the Fermi constant. If G_F is known, we can find the value of g_w using $m_W = 80.385 \pm 0.015 \text{GeV}/c^2$ [8].

One thing concerning the lifetime would be the ratio of muons and anti-muons at sea level. The muons generated in particle cascade inherit the property of their progenitors that are positively charged. This ratio $N(\mu^+)/N(\mu^-) = 1.25$ can be roughly estimated from two reaction channels of cosmic-ray photons in the atmosphere. At sea level this parameter is measured by Burnett et al.(1973) and their result is 1.261 ± 0.009 [9]. Thus the intensity of muons can be decomposed to two

parts,

$$\begin{aligned}
 I(t) &= \frac{N(\mu^-)}{N(\mu^-) + N(\mu^+)} I_0 e^{-t/\tau_-} + \frac{N(\mu^+)}{N(\mu^-) + N(\mu^+)} I_0 e^{-t/\tau_+} \\
 &= 0.44 I_0 e^{-t/\tau_-} + 0.56 I_0 e^{-t/\tau_+}.
 \end{aligned}
 \tag{7}$$

Considering the muon captures, τ_- is lightly smaller than τ_+ . In this experiment, we measured the mean lifetime of muons.

Above all, the measurements of mean speed and lifetime of cosmic muons has deeply strengthened our understanding of relativistic effects for high speed particles and the nature of weak interactions. In this paper, we also tried to elucidate these profound and far-sighted theories through our experiment. This paper is arranged as follows: section two is mainly about the methodology, we will introduce the principles used to measure the speed and lifetime of muons as well as the equipments in our experiment. A brief introduction to Monte Carlo simulations of event-collection efficiency is also included in this section. We present our results and discussions in section three. Conclusions can be found in section four.

II. METHODS AND EQUIPMENT

II. 1 Mean Speed of Muons

II. 1. 1 Principles

The basic idea of measuring the mean speed of muons is straight forward: speed is the distance divided by the time cost to travel. The sketch of our equipment is shown in Fig 8 in appendix B. In our experiment, we used two ‘‘paddles’’ of Bicron BC-408 scintillator deployed on a vertical frame as the detector of muons. When muons hit the photomultiplier tubes (PMT) inside the paddles, one pulse will be triggered. If one muon penetrates both the upper and bottom paddles (we call it an event or a count), the time difference between two pulses should be the duration of the trip between the paddles. The distance is adjustable, which enables us to measure the time differences of different separations. After the pulses are generated, they are sent to the coincidence-analysis system. Details pertaining the setup in this system can be found in appendix B. One vital procedure would be the calibration: find the transformation function from channels to time differences. We will leave the calibration to the end of this section.

When we receive the signal from MCA, the time difference Δt is known. In this experiment,

$$\Delta t = \frac{d}{v_\mu} + t_0 \tag{8}$$

where d is the distance between two paddles and t_0 is the time delay in the cable. In other words, $d = (\Delta t -$

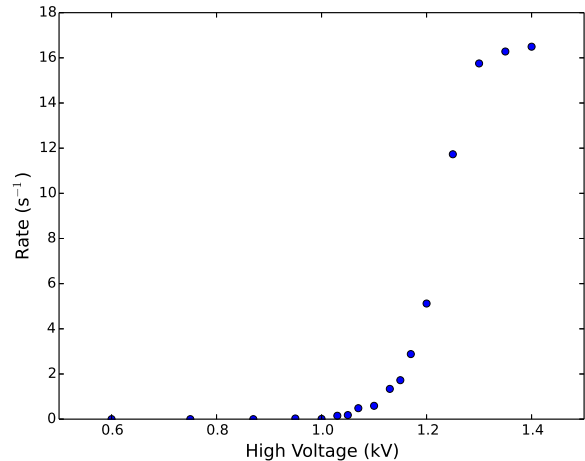


FIG. 3. Counting rate as a function of high voltages for both PMTs. The inflection point is about 1.15kV.

$t_0)v_\mu$ means the speed is the slope in $d - \Delta t$ figures and the measurement of t_0 is not required (in fact, we can determine t_0 from the intercept of d -axis).

In order to optimize the parameters of these devices, an estimate of event rate for different d is very useful. One conventional assumption about the spatial distribution of muons is that intensity only depends on the zenith angle θ and is isotropic in azimuthal direction (ϕ in spherical coordinates). The total muon intensity at sea level varies like

$$I(\theta) = I_0 \cos^2(\theta) \tag{9}$$

where $I_0 = 0.83 \times 10^{-2} \text{cm}^2 \text{s}^{-1} \text{sr}^{-1}$ is the normalized coefficient[10]. For a horizontally placed plate, the total collection rate is

$$\frac{dN}{dt} = \int I_0 \cos^2(\theta) dA d\Omega = \frac{2\pi}{3} A I_0, \tag{10}$$

where A is the area of the plate. In this experiment, the dimension of PMT paddles is $31.50 \text{cm} \times 31.50 \text{cm}$, thus the arrival rate of muons is approximately 17s^{-1} . To estimate the counting rate (depends on d), we ran a Monte Carlo simulation (details can be found in appendix C). From this simulations, we found the time increases linearly with the slant range. This result is quite reasonable because when d increases, the solid angle decrease as well as the efficiency which is evaluated by counts/ N .

II. 1. 2 Calibration

One vital step is to find the converting function between channels from MCA and time differences. Before that, we used the Timer and Counter to find the optimal voltages for PMT by recording the counting rate as a function of voltage when two paddles are overlapping[11].

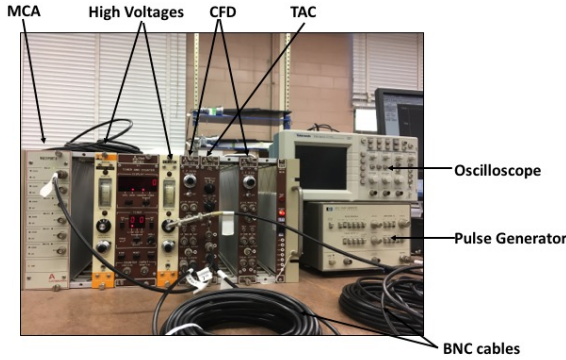


FIG. 4. Setting for calibration. The pulse generator is used as the source of input signals. The time differences are generated by varying the length cables. To check the time difference, we fed the signals from two separated cables to Input 1 and Input 2 in the oscilloscope. The corresponding bin number can be obtained from Genie 2000 after digitalized by MCA.

Our data is shown in figure 3. The best voltage would be 1.15kV (inflection point in this figure) for both upper and bottom PMTs to minimize the spurious signals.

The connection and setup for calibration are shown in figure 4. In this step we need to use a pulse generator as the signal source and an oscilloscope to check the frequency and period of inputs. Here we consider the time delay in BNC cables and use the combination of cables, for example 30', 50', 80', 100' and 130', to get different time differences. For each group, the time difference can be read in the oscilloscope and the channel (bin) number can be obtained from Genie 2000. Thus, we established the correlation between the bin numbers and time differences (please refer to the FIG 5). Using linear function to fit these points, we obtain the convert function from bins to time differences:

$$t = 0.0120 \text{ ns} \times (\text{bins} + 375.51), \quad (11)$$

which is then applied to calculate the speed of muons. In this step, the oscilloscope should be externally terminated into 50 ohms. The key reason is that 50 ohms terminal level is enough to minimize the effect on the pulse generator.

II. 2 Mean Lifetime of Muons

In this experiment, we used a 55-gallon drum of liquid scintillator to collect muons. The setting can be found in figure 6. According to Bethe-Bloch equation[12], when muons are traveling through a medium, they will lose their energy until getting rest. The radiation in this process is detectable. Because the energy-loss time is in magnitude of several *ns* which is much shorter than the lifetime of muons, we can assume the muon is at rest when they emit the stopping signal. Shortly, the muon will

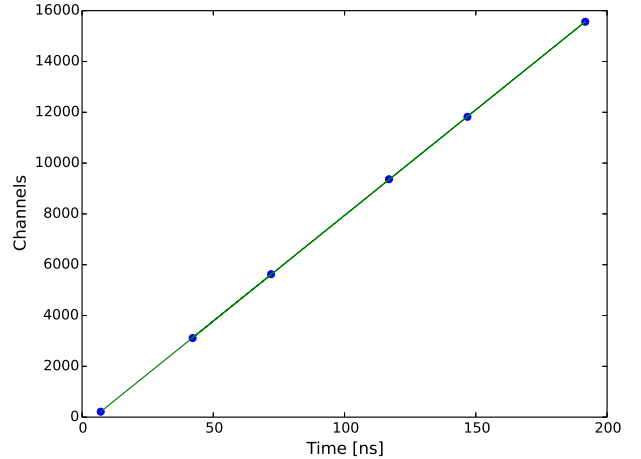


FIG. 5. The relationship between channel (or bin) numbers and time differences. We use the combination of cables to get the time differences. From left to right, the corresponding cable lengths are 30', 50', 80', 100' and 130' respectively. The slope and intercept of linear-fitting function are 83.17 ns^{-1} and -375.51 .

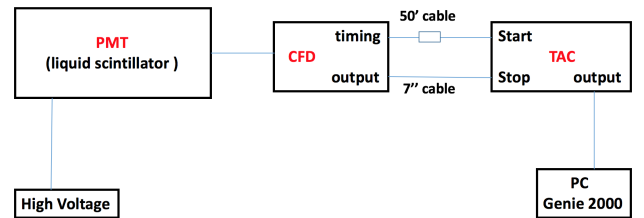


FIG. 6. Setting for lifetime measurement. Here, we use one PMT to generate both pulses and we use a long delay cable to avoid triggering the START and STOP simultaneously. In this circuit, the voltage on PMT is 1.1kV.

decay and generate a relativistic electron whose speed exceeds the light speed in the medium.

The PMT will detect the Cherenkov radiation from the electron. The time difference between these two pulses Δt is related to the intensity, $I_0 e^{-\Delta t/\tau}$. So we can extract the τ from the distribution of Δt . However, we cannot get a perfect exponential decay function in realistic experiment mainly for two reasons. The first one is time delay in the cable t_0 , so the real time difference between stopping and decaying is $\Delta t_m - t_0$, where t_m is the measured time difference. This effect can be considered as a modification to the coefficient I_0 , say $I(\Delta t_m) = I_0 e^{t_0/\tau} e^{-\Delta t_m/\tau}$. Another contribution is attributed to accidental delayed coincidences between random pulses which contribute a uniform background to the counts. As a consequence,

the distribution of Δt_m dumps exponentially at first and then maintain a constant. Therefore, the final distribution is

$$I(\Delta t_m) = I_0 e^{t_0/\tau} e^{-\Delta t_m/\tau} + b. \quad (12)$$

One crucial step in this measurement is choosing the appropriate range on the TAC and threshold on the CFD. In our experiment, they are $100ns \times 100$ and 0.5 respectively. If the threshold is too low, the rate of accidental coincidences is so high that the real events are overwhelmed by the noise, or, most of the decaying events are rejected.

III. RESULTS AND DISCUSSION

III. 1 Measurement of Mean Speed of Muons

To measure the speed of muons, we adjusted the vertical position of paddles to get six different separations: 20 cm, 50 cm, 84 cm, 95 cm, 151 cm and 190 cm. The distributions of count for different separations were fitted by Gaussian function (see appendix D). Using the previous convert function (equation 11), we got the relation between the separations d_i and time differences Δt_i . From Equation 8, we found the speed of muons is the slope of the linear function in $\Delta t - d$ plane (as shown in FIG 7). The average speed obtained from least square method is $1.583 \pm 0.011 \times 10^8 \text{ m s}^{-1}$. This value is 52.77% of the speed of light which indicates that the upper limit on the relative speed of inertial frames holds. However, our result of muons' speed is much lower than reported results (about 99% c)[13][14].

This discrepancy mainly came from the malfunction of our apparatus instead of the low speed of muons. In fact, we double-checked our setups and procedures for several times and we came to the conclusion that the TAC is malfunctioning. The evidences are presented as follows. The CFD is designed to mimic the mathematical operation of finding a maximum of a pulse which converts the pulses from PMT to processable inputs for TAC. Since the distributions of events are correct (see FIG 11 to FIG 16) and correlation between d and Δt is a well-define linear function, we concluded that the CFDs worked well. However, the internal failure of TAC will produce the false time-to-amplitude signal. At the beginning, we tried to calibrate through changing the period of pulse generator, but the bins we got on Genie 2000 are random. Therefore, it is more possible that there is something wrong with TAC which causes the incorrectness of calibration.

If the TAC is not faulty, we are expected to get a lower time-per-bin value. In our calibration, each bin represents $t_0 \approx 0.012ns$ instead of $t_0 \approx 0.007ns$ as found in the manual. Using the correct value, the speed is $2.71 \times 10^8 \text{ m/s}$ (90% c) which is very close to the speed of light. If a speed of 99% c is measured, the Lorentz factor would be $\gamma = 1/\sqrt{1 - (v/c)^2} \approx 7.1$. Therefore, the time

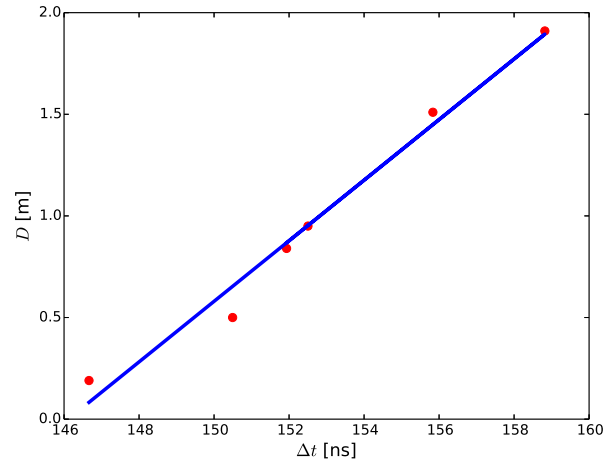


FIG. 7. separations v.s. time differences. The speed of muons, $1.583 \times 10^8 \text{ m s}^{-1}$, is estimated using least square method (blue solid line) with the relative standard error to be 0.7%.

that muons can travel in laboratory frame is $t_L = \gamma\tau$ where τ is the mean life time and the energy can be up to the magnitude of giga-electron volts. On the other hand, the detectability of atmospherical muons indicates their speed is very close to c .

III. 2 The Failed Muon Lifetime Measurement

Eventually, we failed to measure the mean life time of muons because of the faulty apparatus. In our experiment, the TAC is possibly malfunctioning. The reason is that the basic principles of calibration and measurement of life time are very analogous and the success of this experiment relies highly on TAC to convert the time difference from CFD to amplitude. If the STOP and START signals are not separated correctly, we cannot get any meaningful results from Genie 2000 except white noise. Since we can get some useful patterns in the speed measurement, for instance, the linear relation between d and Δt (see FIG 7) and the Gaussian distributions of events (see FIG 11 to FIG 16), it is reasonable to conclude that CFDs and MCA are working regularly and it is the TAC where the problem exists.

If the apparatus are working well, we are expected to get a distribution of time differences with an exponentially decreasing feature as described in equation 12. Then, using the function

$$\text{counts} = A \times \exp\left(-\frac{t}{\tau}\right) + B \quad (13)$$

to fit this distribution, we can get the mean lifetime τ (here A and B are constants). The widely accepted value from modern measurement is $\tau \approx 2.197 \mu s$ [15]. The proper time interval of the frame in which muons are

at rest is given by $\Delta t = s/(\gamma v)$, where s is the distance the muons travel. With this time, the survival rate of muons is

$$\frac{P(s)}{P(0)} = \exp\left(-\frac{L}{\gamma v \tau}\right). \quad (14)$$

Substituting $\gamma = 7.1$, $\tau = 2.197\mu s$, $v = 0.99c$ and $s = 15\text{km}$ into this equation, we obtain the survival probability at sea level is $\approx 4.1\%$. Consider a tremendous number of muons are generated in the atmosphere, the incident rate at sea level is still observable.

IV. CONCLUSIONS

In this experiment, we attempted to measure the speed and lifetime of sea-level muons using our PMTs and coincidence-analysis system. Because of the faulty apparatus, we cannot get correct values. Despite of that, we provided the valid methods to calibrate and to measure the speed and lifetime. We proved that we must consider the relativistic dilation when studying the propagation of muons and that muons are observable at sea level by calculating the survival probability. Moreover,

using $\tau = 2.197\mu m$, we estimated the weak coupling constant to be $G_F \approx 1.167 \times 10^{-5} \text{GeV}^{-2}$, which is consistent with[8].

After carefully checking each part of the apparatus, we concluded there are some problems with TAC. If everything went as expected, the speed of muons can be measured up to 99% of light speed that reveals an upper limit of speed, which is one of the fundamental assumptions of special relativity. In addition, as we can find from our calculations, the Classical Mechanics is invalid in high-speed situations where relativistic theory governs the motions.

ACKNOWLEDGMENTS

I am especially grateful to our instructor, Prof. Mauricio Terrones, and our teaching assistant, Mr. Zhong Lin, for numerous technical suggestions and careful reading of the previous version of this paper. Thanks also to my partner, Mr. Ding Ding, for his everlasting endeavor and patience towards the experiment. This work is supported by the Department of Physics of the Pennsylvania State University.

-
- [1] S. Hayakawa, *Cosmic Ray Physics* (Wiley Interscience, New York, 1969).
 - [2] C. Grupen, *Astroparticle Physics*, SpringerLink: Springer e-Books (Springer, 2005).
 - [3] *Nobel Prize in Physics 1936: Presentation Speech* (1936-12-10).
 - [4] B. C. Rastin, *Journal of Physics G: Nuclear Physics* **10**, 1609 (1984).
 - [5] K. A. Olive *et al.* (Particle Data Group), *Chin. Phys.* **C38**, 090001 (2014).
 - [6] S. H. Neddermeyer and C. D. Anderson, *Phys. Rev.* **51**, 884 (1937).
 - [7] M. Thomson, *Modern Particle Physics* (Cambridge University Press, 2013).
 - [8] J. Beringer *et al.* (Particle Data Group), *Phys. Rev. D* **86**, 010001 (2012).
 - [9] T. H. Burnett *et al.*, *Phys. Rev. Lett.* **30**, 937 (1973).
 - [10] B. Rossi, *Rev. Mod. Phys.* **20**, 537 (1948).
 - [11] *Muon Speed and Lifetime*, Department of Physics, Pennsylvania State University.
 - [12] H. Bethe and J. Ashkin, *Experimental Nuclear Physics* (Wiley, New York, 1954).
 - [13] B. C. Vest *et al.*, *Wabash Journal of Physics* **1**, 1.3 (2010).
 - [14] N. A. Romero and M. T. Vengalattore, MIT Lab paper (1998).
 - [15] D. M. Webber *et al.* (MuLan Collaboration), *Phys. Rev. Lett.* **106**, 041803 (2011).

Appendix A: Lorentz transformation

The transformation from two inertial frames, say S (in which muons are at rest) and S' (laboratory frame), is given by

$$\begin{pmatrix} x' \\ y' \\ z' \\ ict' \end{pmatrix} = \begin{pmatrix} \gamma & 0 & 0 & i\beta\gamma \\ 0 & 1 & 0 & 0 \\ 0 & 0 & 1 & 0 \\ -i\beta\gamma & 0 & 0 & \gamma \end{pmatrix} \begin{pmatrix} x \\ y \\ z \\ ict \end{pmatrix}, \quad (A1)$$

where $\beta = v/c$, $\gamma = 1/(1 - \beta^2)^{1/2}$ and v is speed of S' in S .

Appendix B: Setup for speed measurement

After the pulses are generated in PMTs, they are sent to the Constant-Fraction-Discriminator (CFD) separately. If the input signal satisfies the requirements: the fast negative signal is in the range $-5V \sim 0$, two timing-output connectors will provide simultaneous fast negative signals (these two signals are useful in the calibration). Now we feed the signals from two CFDs to the Time-to-Amplitude Converter's (TAC) START and STOP connectors. TAC can convert the time difference between START and STOP signals into an outgoing voltage pulse. The amplitude of output signal typically varies in the range $0 \sim 10V$ and is proportional to the time difference. Because the START-to-STOP time conversion

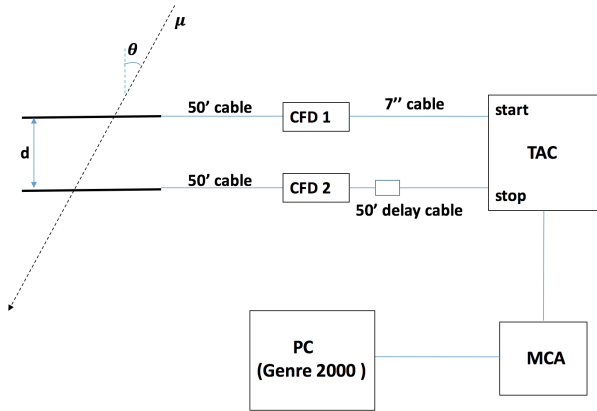


FIG. 8. Arrangement for measuring the mean speed of muons. θ is the zenith angle and d is the separation of two paddles. The dashed is the trajectory of incident muons. In this experiment, the delay cable between CFD and TAC STOP Input is chosen to be 50'.

is accomplished only after the START has been identified after a STOP pulse has arrived within the selected range. One important step to avoid the overlap of START and STOP signals would be adding a 50' delay cable between the CFD and the stop connector on TAC (see figure 8). In order to choose the correct range, we roughly estimated the upper limit of Δt , which is 10ns, if the largest separation between two paddles is chosen to be 3m. Considering the delay in the cable, 100ns is a reasonable choice for the range. The output pulse of TAC is digitized by the Multichannel Analyzer (MCA). The pulse are counted based on the amplitude and the amplitude is converted to the number of channels. Through all of these procedures, the time difference between two paddles are finally converted to the channels which is analyzable in the PC software Genie 2000 and the relation between time differences and channels/bins is established through these devices.

Appendix C: Monte Carlo Simulations of Event Rate

In our code, the distribution of x , y coordinates and ϕ on the upper paddle is uniform. And we use the following rules to simulate the distribution of θ :

- (i) Generate a random number ξ which is uniformly distributed in $[0, 1)$;
- (ii) Generate a random number θ_s which is uniformly distributed in $[0, \pi/2)$;
- (iii) If $\cos^2(\theta_s) \geq \xi$, this zenith angle is accepted, otherwise go to the step (i).

Once the "muon" is generated in the upper paddle, we will track its propagation and determine whether this "muon" can reach the bottom paddle. Repeat these procedures for many time until the counts equal 100, we get figure 9. In addition, we estimate the time for collecting

1000 counts at different slant ranges in the unit of the time t_0 for $d = 0$. Our result is shown in figure 10.

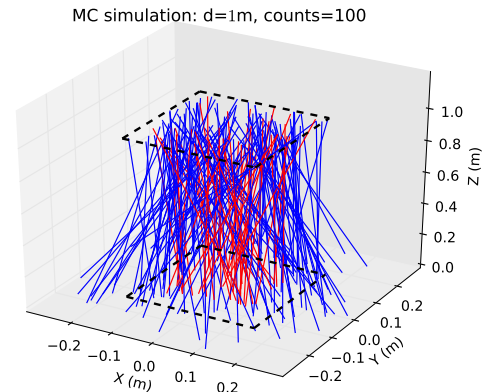


FIG. 9. Monte Carlo simulations for the slant range $d = 1\text{m}$. The trajectories of muons which intrigue the counts are shown in red while failed muons are illustrated in blue. The count is fixed to be 100

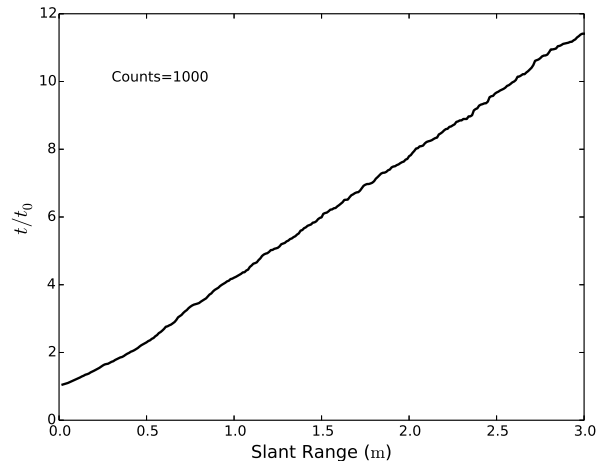


FIG. 10. An estimate of waiting time for 1000 counts of different d . t_0 is the time required when two paddles are overlap ($d = 0$).

Appendix D: Muon speed measurements

The distribution of counts of different separations are fitted using Gaussian function,

$$\text{count} = A \times \exp \left[-\frac{(\text{channel} - x_0)^2}{\sigma^2} \right] + B, \quad (\text{D1})$$

where x_0 is the center of the peak, σ is the standard deviation, A and B are constants. The results of six

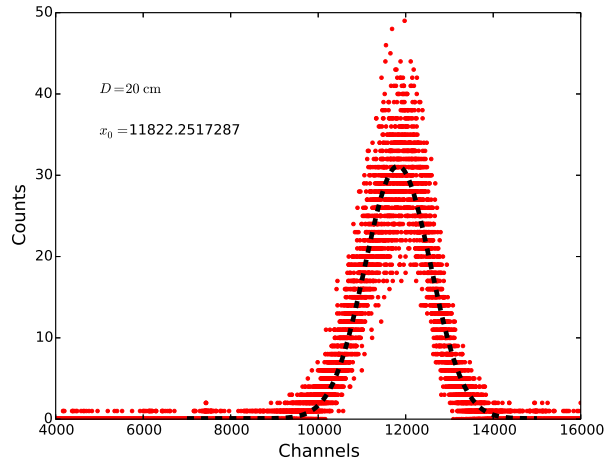


FIG. 11. 20 cm separation: the peak is $x_0 = 11822.2517287$. Point: original data, dashed line: fitting function.

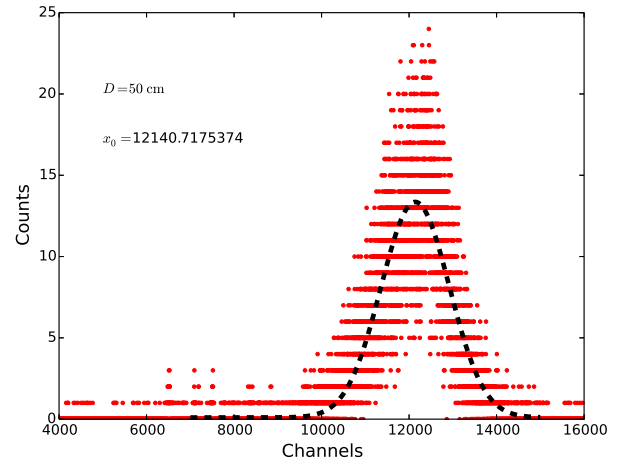


FIG. 12. 50 cm separation: the peak is $x_0 = 12140.7175374$. Point: original data, dashed line: fitting function.

separations (20 cm, 50 cm, 84 cm, 95 cm, 151 cm and 190 cm) are illustrated in FIG 11 to FIG 16.

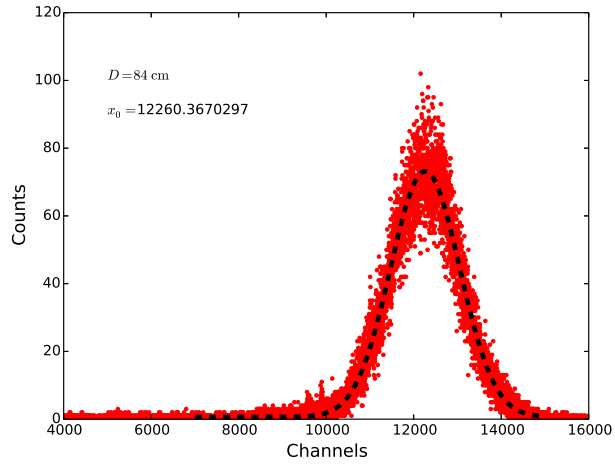


FIG. 13. 84 cm separation: the peak is $x_0 = 12260.3670297$. Point: original data, dashed line: fitting function.

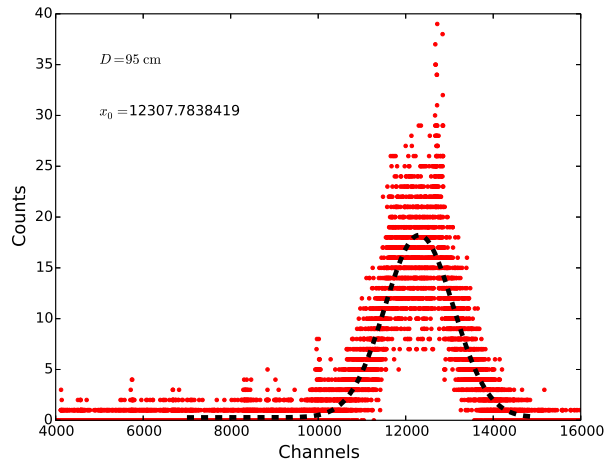


FIG. 14. 95 cm separation: the peak is $x_0 = 12307.7838419$. Point: original data, dashed line: fitting function.

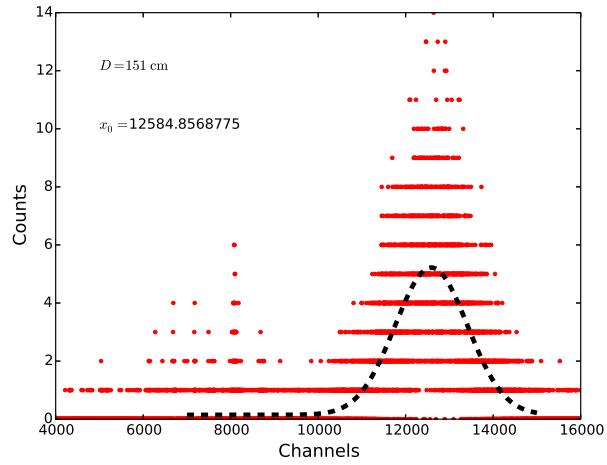


FIG. 15. 151 cm separation: the peak is $x_0 = 12584.8568775$.
Point: original data, dashed line: fitting function.

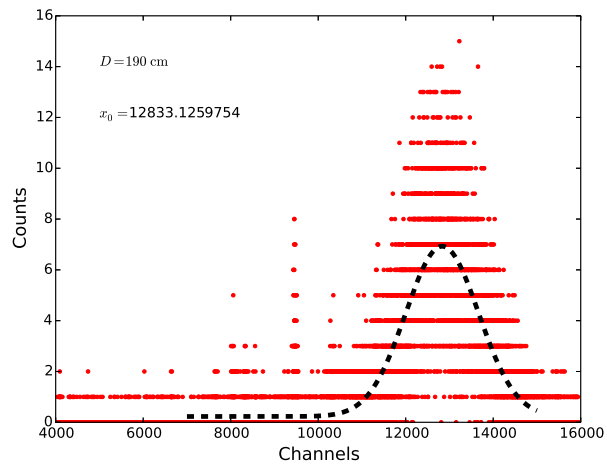


FIG. 16. 190 cm separation: the peak is $x_0 = 12833.1259754$.
Point: original data, dashed line: fitting function.